CONF-9505122--199 SLAC-PUB-95-6900
May 1995

IMPEDANCE ANALYSIS OF THE PEP-II VACUUM CHAMBER*

C.-K. Ng and T. Weiland†
Stanford Linear Accelerator Center, Stanford University, Stanford, CA 94309

Abstract

The PEP-II high energy ring (HER) vacuum chamber consists of a copper tube with periodically spaced pumping slots. The impedance of the vacuum chamber due to the slots is analyzed. Both narrow-band and broad-band impedances are considered as well as longitudinal and transverse components thereof. It is found that although the broad-band impedance is tolerable, the narrow-band impedance may exceed the instability limit given by the natural damping with no feedback system on. Traveling wave modes in the chamber are the major source of this high value narrow-band impedance. We also study the dependences of the impedance on the slot length and the geometrical cross section.

I. ABOUT *SMALL* IMPEDANCES

In oder to create a "feeling" about the magnitude of *small* impedances, we shall start with a general note of caution showing that even a tiny little cavity in a beam pipe can easily create kΩ of impedance. Thus one such small cavity by itself might be capable of driving the beam unstable. Let us consider for simplicity a circular symmetric beam pipe with a small pill-box cavity in it. Such a cavity (see Fig. 1) has one trapped mode [1] for each m, where m is the azimuthal mode number. We restrict our consideration to the TM_{010} mode here for simplicity and obtain by numerical analysis with MAFIA the trapped mode as shown in Fig. 2. The trapped mode parameters are listed in Table 1. It can be seen that a tiny cavity with only 3 mm dent at the outside of the beam pipe can exceed the tolerable impedance limit in a B-factory machine without feedback by a significant factor. A deeper dent of 10 mm over the length of 20 mm is even 12 times higher and becomes relevant even if there is a powerful feedback.

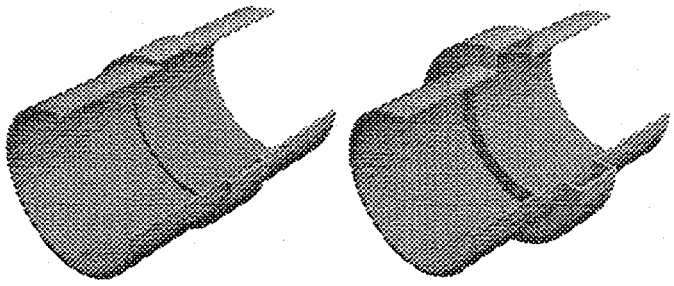

Figure 1. Three dimensional cutaway view of two very small cavities in a circular beam pipe. The cavity is 20 mm long. Their inner radius is 35 mm, and the outer radii are 38 mm and 45 mm for the two cases.

*Work supported by the Department of Energy, contract DE-AC03-76SF00515.

†Permanent address: University of Technology, FB18, Schlongortenstr.8, D64289, Darmstadt, Germany.

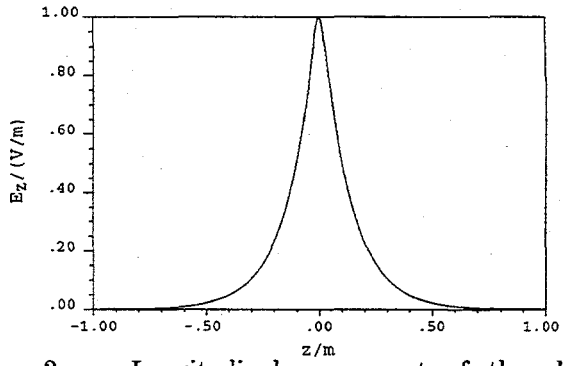

Figure 2. Longitudinal component of the electric field of the trapped mode TM_{010} in a small "cavity" (r_{outer}=45 mm) in a circular beam pipe. Note the exponential decay over a long distance at both sides.

Gap length (mm)	20	20
r_{inner} (mm)	35	35
r_{outer}	38	45
f_{res} (GHz)	3.258	3.062
R_s (kΩ)	7	88
Q	27000	20000
k_0 (V/pC)	0.003	0.042

Table 1: Small cavity trapped mode parameters.

II. VACUUM CHAMBER MODELS

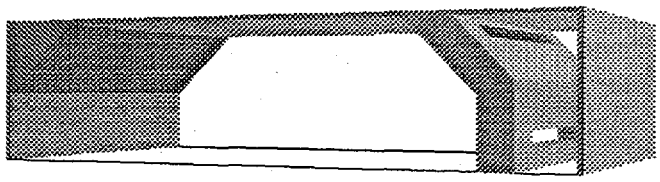

Figure 3. Three dimensional view of a generic vacuum chamber model with four pumping slots connecting the beam chamber with a side chamber. The side chamber houses vacuum pumps. For the purpose of impedance analysis the pumps are replaced by a conducting wall. The inner width is 9 cm, the inner height 5 cm, the slot width 3 mm, and the longitudinal slot spacing 1 cm. The only free parameter is the slot length L_{slot} and the number of slotted sections.

Various models of the vacuum chamber have been analyzed for PEP-II. However, as the basic physical picture is the same for all the different models, only a generic one is considered here. Fig. 3 shows the three-dimensional view of a generic vacuum chamber with slots on one side. The dimensions have been chosen close to the PEP-II design[2], but may be considered as a generic chamber layout for electron/positron storage rings. Actually, the vacuum chamber of PEP, PETRA and HERA are almost identical in size.

Presented at the 16th IEEE Particle Accelerator Conference (PAC 95) and International Conference on High Energy Accelerators, Dallas, Texas, May 1-5, 1995

All results presented here are per vacuum chamber slotted section and not for the full length of the final chamber. Thus depending on the slot length one has to multiply the single section results with an appropriate factor. For PEP-II this factor is approximately $1000/L_{slot}$(m).

III. LONGITUDINAL BROAD-BAND IMPEDANCE

The impedance in general depends on the slot length and it saturates when the length is about 1-2 times of its width [3]. The pumping requirements normally only are set by a total pumping channel cross section. Thus it is worthwhile to investigate the influence of the length of a slot in order to find an optimum slot length from the impedance point of view. The wakefield is found to be purely inductive in nature. From the low frequency spectrum of the wakefield, the inductance is determined and its length dependence is shown in Fig. 4. The inductance converges very quickly to a saturated value of 4.0×10^{-5} nH. The loss parameter has similar variation behavior and its saturated value is 7.9×10^{-7} V/pC. This parameter is a good indication of the effective real part of the impedance weighted with the bunch spectrum. The real part of the impedance is obviously rather small compared to the imaginary part.

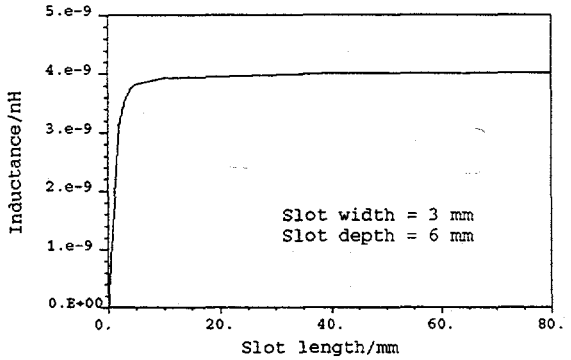

Figure 4. Inductance as a function of slot length.

IV. LONGITUDINAL NARROW-BAND IMPEDANCE

Narrow-band impedances are mostly locally confined resonant modes in cavities. A second type of resonant impedance is given by the waveguide character of a vacuum chamber. Basically being a periodic structure, it carries traveling waves with longitudinal and transverse modes just like any traveling wave accelerating structure. There are two possibilities to address this particular impedance, namely frequency and time domain approaches. Strong effects may be found by time domain simulations of a few sections, and weaker effects by modeling the chamber as a periodic structure in frequency domain.

(a) *Section-to-section resonant effects*

In order to identify strong section-to-section effects the wake potentials were computed for pieces consisting of 1,2,4 and 8 sections, with 4 slots per section (see Fig. 3). On the scale where the wake potential is inductive, no significant build-up of a resonant type of impedance has been observed. However, this does not mean that the resonant impedance is negligible but only that it is small compared to the inductive broad-band impedance. Very narrow impedances cannot be found this way but need to be analyzed by frequency domain approaches.

(b) *Traveling Wave Analysis*

As a single mechanical unit, a vacuum chamber is made from 100-200 sections, and an analysis based on infinitely repeating structure is adequate. Thus we can compute traveling waves for any given phase advance per cell. Such a computation results in a Brillouin diagram as one normally finds in linear accelerator designs where similarly long structures (100-200 cavity cells) are used in one unit.

For the vacuum chamber there exist two types of modes. One group shows almost "empty waveguide" mode patterns. A second group shows fields concentrated in the slot region with almost no field in the center of the vacuum chamber. Examples of these modes for 40 mm slot length are shown in Figs. 5 and 6. In Fig. 7, we show the Brillouin diagram for the structure. The loss parameters, quality factors and shunt impedances for the first seven synchronous waves are listed in Table 2. The mode shown in Fig. 6, a TM_{11}-like mode, has a strong beam coupling. Its impedance is comparable to the acceptable value.

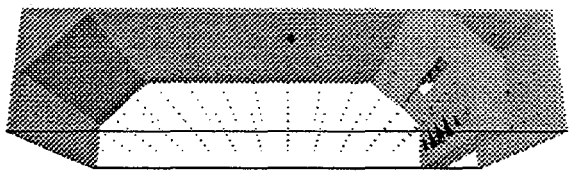

Figure 5. The real part of the electric field of mode 2 with $f = 3.616$ GHz and phase advance 120° per section.

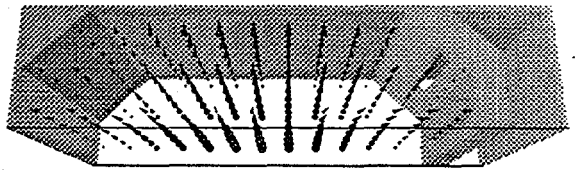

Figure 6. The real part of the electric field of mode 4 with $f = 3.996$ GHz and phase advance 120° per section.

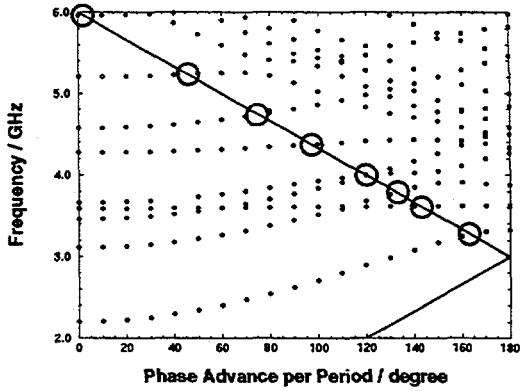

Figure 7. The Brillouin diagram for the vacuum chamber with a slot length of 40 mm and a period length of 50 mm. The line light is the solid straight curve. The synchronous modes are marked by circles.

Mode	ϕ /°	f/GHz	k/(V/C)	Q	$R_s/m\Omega$
1	163	3.27	1892	5000	1
2	143	3.63	383	35000	1
3	133	3.80	20170	15000	25
4	120	4.00	148000	27000	318
5	120	4.00	3129	8000	2
6	97	4.37	8129	10000	6
7	75	4.74	23960	37000	60

Table 2. First seven synchronous modes and the associated impedances, quality factors, loss parameters and shunt impedances.

V. TRANSVERSE BROAD-BAND IMPEDANCE

Since the vacuum chamber is symmetric with respect to the horizontal axis, the vertical forces vanish exactly when the particles pass the chamber on axis. In the horizontal plane the situation is more complex. As there is no right-left symmetry in the vacuum chamber, transverse wake forces act on the particles all the time, wherever they pass with respect to the center of the chamber. The impedance is split into a constant and x-dependent part. These portions can be obtained by computing the wake potentials at different horizontal beam positions. The difference of the wake potentials between off-axis and on-axis divided by the offset gives an impedance compatible with the standard theory for transverse impedances. The constant remaining part and the linearly rising part of the wake potentials have different effects on the beam dynamics. The vertical and horizontal components of the transverse wake potential are shown in Fig. 8.

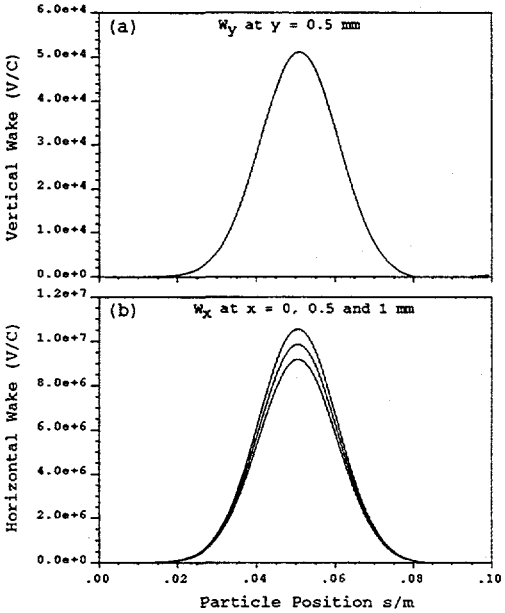

Figure 8. Transverse wake potentials as functions of s.

The effects of the transverse wakes can be evaluated by the effective transverse kick parameter defined as $k_\perp = \int_{-\infty}^{\infty} \rho(s) w_\perp(s) ds / (\int_{-\infty}^{\infty} \rho(s) ds)^2$. The horizontal and transverse $k_\perp$ are found to be 0.00087 and 0.00003 V/pC/m respectively. The horizontal $k_\perp$ is higher because of the large non-varying part of the wake potential. For a typical single-cell 500 MHz cavity, $k_\perp \sim 3$ V/pC/m. Thus the transverse kicks of the vacuum chamber have very small effects on beam dynamics properties such as tune shift.

VI. TRANSVERSE NARROW-BAND IMPEDANCE

One of the first traveling wave modes mentioned in section IV is investigated here as an example, being likely a candidate for a strong transverse narrow-band impedance. The fields are shown in Fig. 9. The longitudinal loss parameter as a function of horizontal position is shown in Fig. 10. The transverse impedance of this mode is found to be 0.134 MΩ/m^2, which should be compared with 340 MΩ/m^2 of a typical single-cell 500 MHz cavity.

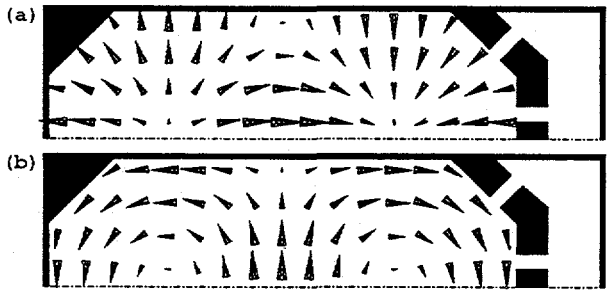

Figure 9. Real part of the (a) electric; (b) magnetic field of mode 7 (f=4.737 GHz) at the synchronous phase of 75°.

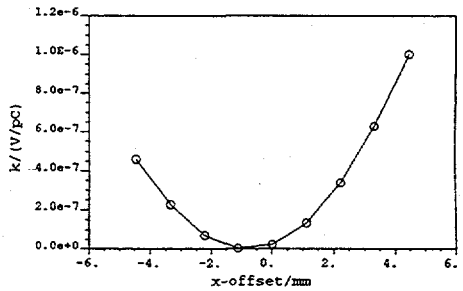

Figure 10. The longitudinal loss parameter as a function of horizontal position x. The functional dependence is nearly quadratic. Due to the mechanical asymmetry, the minimum of the wake is not at the center x=0, but is slightly shifted away from the slotted side of the vacuum chamber.

VII. DISCUSSIONS

The broad-band and narrow-band impedances can be further reduced by orders of magnitude by using hidden slots [4] embedded half-way in a continuous longitudinal groove. In fact, the PEP-II design has chosen this approach. Furthermore, the effects of transverse impedances on beam dynamics remain to be investigated.

Acknowledgements

We thank A. Chao, E. Daly, S. Heifets, G. Lambertson, M. Nordby and G. Stupakov for useful discussions.

References

[1] T.Weiland, Single Mode Cavities - A Possibility for Fighting Collective Beam Instabilities, DESY Vol. 83(073), Sep 1983.

[2] An Asymmetric B Factory, Conceptual Design Report, LBL-PUB-5379 or SLAC-418, June 1993.

[3] K. L. F. Bane and C.-K. Ng, Impedance Calculations for the Improved SLC Damping Rings, Proc. 1993 PAC, p3432.

[4] T. Weiland, Low impedance Vacuum Chambers, PEP-II Technical Note No. 59, 1994.

DISCLAIMER